

***Ab initio* calculations of inelastic losses and optical constants**

J. J. Rehr,¹ J. J. Kas,¹ M. P. Prange,¹ F. D. Vila,¹ A.

L. Ankudinov,¹ L. W. Campbell,² and A. P. Sorini¹

¹*Department of Physics, University of Washington, Seattle, WA 98195*

²*Department of Physics, State University of New York, Geneseo, NY 14454*

(Dated: September 17, 2018)

Abstract

Ab initio approaches are introduced for calculations of inelastic losses and vibrational damping in core level x-ray and electron spectroscopies. From the dielectric response function we obtain system-dependent self-energies, inelastic mean free paths, and losses due to multiple-electron excitations, while from the dynamical matrix we obtain phonon spectra and Debye-Waller factors. These developments yield various spectra and optical constants from the UV to x-ray energies in aperiodic materials, and significantly improve both the near edge and extended fine structure.

PACS numbers: 78.20.Ci, 78.70.Dm, 82.80.Pv

Theories of x-ray and electron spectra and other “optical constants” have become increasingly sophisticated [1, 2]. For example, treatments of such spectra can now go beyond the independent-particle approximation, e.g., with time-dependent density functional theory (TDDFT) or the Bethe-Salpeter equation (BSE) [3, 4]. However, less attention has been devoted to the effects of inelastic losses and vibrational damping, especially at high energies. These losses are important both in spectroscopy and other applications [5, 6]. Thus current treatments [2, 7, 8] often utilize simplified models, e.g., semi-empirical or electron-gas self-energies and Einstein or Debye models for vibrations, with considerable variations in the results.

To address these difficulties we introduce in this Letter *ab initio* approaches for these many-body damping effects. We first present an approach for calculating the dielectric response and optical properties within a real-space Green’s function (RSGF) formalism [2, 4]. From these results, we derive a many-pole model for the dielectric function, which is then used to obtain photoelectron self-energies, inelastic mean free paths (IMFPs), and contributions from multi-electron excitations. Next, from calculations of the dynamical matrix we obtain phonon spectra and quantitative Debye-Waller (DW) factors. These developments enable a number of applications, e.g., improved calculations of spectra and inelastic losses from the UV to hard-x-ray limits.

A key physical quantity in these calculations is the dielectric response function $\chi(\omega)$ [1]. In the long wave-length limit, various spectra are related to $\chi(\omega)$ through the local atomic polarizability $\alpha(\omega)$ [9],

$$\begin{aligned}\alpha(\omega) &\equiv \int d\mathbf{r}d\mathbf{r}' d^\dagger(\mathbf{r}) \chi(\mathbf{r}, \mathbf{r}', \omega) d(\mathbf{r}) \\ &= \sum_{i,L,L'} \tilde{M}_{i,L} \langle G_{L,L'}(E) \rangle \tilde{M}_{L'i}.\end{aligned}\tag{1}$$

Here, $\tilde{M}_{i,L}$ are screened dipole matrix elements between occupied core states $|i\rangle$ and final scattering states $|L, 0\rangle$, and $G_{L,L'}(E)$ are matrix elements of the photoelectron Green’s function in an angular momentum and site basis [4]. The operator $d(\mathbf{r})$ represents the dipole coupling to the photon field, and the brackets $\langle \cdots \rangle$ denote a configurational average, which can be expressed in terms of DW factors. From $\alpha(\omega)$ we obtain the dielectric constant $\epsilon(\omega) = 1 + 4\pi n\alpha(\omega)$, where $n = N/V$ is the atomic number density [12]. Other optical constants (e.g., absorption coefficient μ , reflectivity \mathcal{R} , anomalous x-ray scattering amplitudes

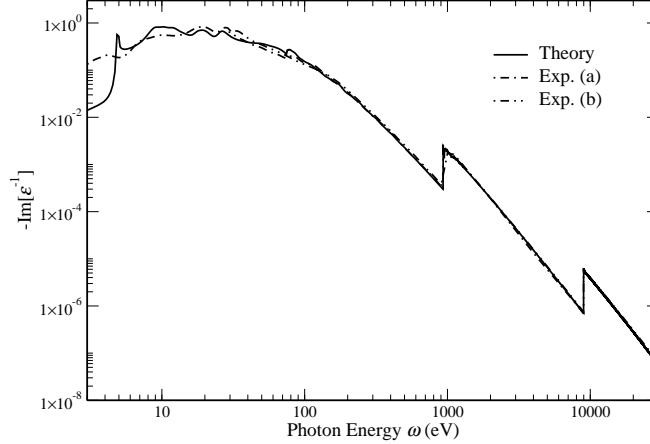


FIG. 1: Energy loss function $-\text{Im}[\epsilon^{-1}]$ for fcc Cu *vs* photon energy ω from this work (solid), and from experiment (a) (dash-dot) [10] and (b) (dash-dot-dot) [11].

$f_1 + if_2$, etc.) are related to $\epsilon \equiv \epsilon_1 + i\epsilon_2$. Typical results, e.g., for the energy loss function $-\text{Im}[\epsilon^{-1}] = \epsilon_2/[\epsilon_1^2 + \epsilon_2^2]$ for Cu (Fig. 1), are in good agreement with experiment [10, 11] in the UV and beyond. This and other examples based on our approach are tabulated on the WWW [13].

The quantities in Eq. (1) are calculated using an extension of our RSGF code [12] that includes corrections to the independent-particle approximation [4]. Compared to other approaches, the RSGF method is advantageous for core-level spectra since it avoids an explicit calculation of energy eigenstates and is applicable to periodic and aperiodic systems alike. For each core state $|i\rangle$, we first calculate the atomic-like background with no scattering; fine structure is then added with full multiple scattering (MS) to about 50 eV, and then with the MS path expansion to about 1500 eV above each edge. In our code both $G(E) = 1/(E - h' + i0^+)$ and the scattering states $|L, 0\rangle = R_L(r)Y_L(\hat{\mathbf{r}})$ are obtained with a self-consistent final-state, muffin-tin Hamiltonian $h' = p^2/2 + V'_{\text{coul}} + \Sigma(E)$. This Hamiltonian includes a screened core-hole, an energy-dependent self energy $\Sigma(E)$, and the core-hole lifetime Γ (we use Hartree atomic units $e = \hbar = m = 1$). Our screened core-hole agrees well with that from the random phase approximation, and gives results for core-level spectra which are a good approximation to the BSE [14]. The screened dipole operators in \tilde{M} account for the induced local dipole fields [9]. For metals, the low-frequency behavior of $\epsilon(\omega)$ is approximated by an additive Drude term; otherwise there are no adjustable parameters.

From the dielectric response, we obtain the self-energy $\Sigma(E)$ using the “GW approxima-

tion” [15],

$$\Sigma(E) = i \int \frac{d\omega}{2\pi} G(E - \omega) W(\omega) e^{-i\delta\omega}, \quad (2)$$

where $W = \epsilon^{-1}(\omega)V$ is the screened coulomb interaction, and matrix indices $(\mathbf{r}, \mathbf{r}')$ are suppressed. For $G(E)$, we use the free Green’s function, ignoring MS terms. Hence our $\Sigma(E)$ represents an *average* self-energy, which is nevertheless adequate for many applications. Current GW implementations for core spectra [2] typically use a single-plasmon pole approximation for the dielectric function. Although computationally efficient, Fig. 1 shows that a single pole may not be a good representation. Thus, to obtain improved self-energies that exploit the efficiency of pole models, we match our *ab initio* $\epsilon(\omega)$ to a many-pole model, with poles spread over a broad spectral range,

$$-\text{Im} [\epsilon^{-1}(\mathbf{q}, \omega)] = \frac{\pi}{2} \sum_j g_j \omega_j \delta(\omega - \omega_j(\mathbf{q})). \quad (3)$$

Here $g_j = (2\Delta\omega_j/\pi\omega_j) \text{Im}[\epsilon^{-1}(\omega_j)]$ is the strength of pole j and $\Delta\omega_j$ is the pole spacing. For simplicity, the momentum dependence of each pole is approximated by a polynomial in q^2 : $\omega_j(\mathbf{q}) = [\omega_j^2 + q^2/3 + q^4/4]^{1/2}$ [16]. This approximation is roughly consistent with explicit calculations [17], but the precise dispersion is not critical since \mathbf{q} and ω are integrated over [16]. Many-pole models [18] and other methods [19] have been developed for more accurate self-energy calculations; however, these methods are computationally demanding and not applicable at high photoelectron energies (e.g., for the extended x-ray absorption fine structure (EXAFS)). Our model is similar to that of Ref. [7], but does not rely on empirical optical constants. Thus using Eq. (3) in Eq. (2), we obtain an efficient approximation for the self-energy as a sum over single-pole models with excitation energies ω_j , i.e., $\Sigma(E) = \sum_j g_j \Sigma(E, \omega_j)$. As an application we have calculated the IMFP $\lambda = (E/2)^{1/2}/|\text{Im}\Sigma(E)|$ for various materials [13]. Fig. 2 shows λ for fcc Cu using a 100-pole model matched to the loss function in Fig. 1. Clearly this model corrects the excessive loss of the single-pole model below 100 eV, and yields quantitative agreement with semi-empirical fits to experiment [5, 20]. Our self-energy is also in reasonable agreement with that of Ref. [18]. A similar approach [21] can be applied to inelastic electron scattering [6] and to photoemission spectra [8].

Our many-pole model also permits calculations of inelastic losses due to multi-electron (e.g. “shake-up” and “shake-off”) excitations. These excitations correspond to satellites beyond the quasi-particle peak in the *spectral function* $A = (-1/\pi) \text{Im} G_{\text{eff}}$. Here G_{eff}

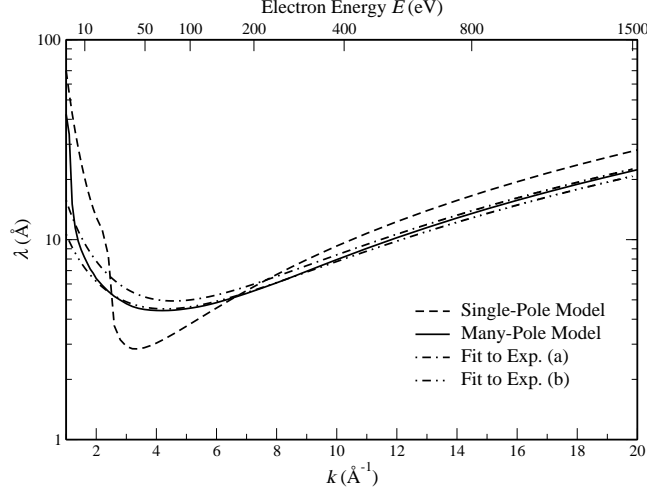


FIG. 2: Inelastic mean free path λ for fcc Cu *vs* electron wave number $k = (2E)^{1/2}$ and kinetic energy E for our many-pole model (solid), a single plasmon-pole model (dashes); and fits to experiment (dash-dots) (a) [20] and (b) [5].

is an effective, one-particle propagator, which can be calculated using a generalization of the GW approximation with similar ingredients [22]. In addition to intrinsic losses, G_{eff} contains energy-dependent interference terms which tend to suppress the satellites. As shown in Ref. [22], these excitations can be included in $\mu(\omega)$ in terms of a convolution of a normalized spectral function \tilde{A} and the quasi-particle absorption coefficient μ_{qp} in the absence of satellites,

$$\mu(\omega) = \int_0^\infty d\omega' \tilde{A}(\omega, \omega') \mu_{qp}(\omega - \omega') \equiv \langle \mu_{qp}(\omega) \rangle, \quad (4)$$

where ω' is the excitation energy. Likewise, the net EXAFS is given by a convolution of \tilde{A} with the quasi-particle fine structure. Thus for each path R in the MS path expansion, the convolution over the oscillatory fine structure yields an amplitude reduction factor $S_R^2(\omega)$ and (since A is asymmetric) a negative phase shift $\delta_R(\omega)$,

$$\langle e^{2ikR} \rangle = S_R^2(\omega) e^{2ikR + \delta_R(\omega)}. \quad (5)$$

For the first shell of Cu, we find that $S_R^2(\omega)$ and $\delta_R(\omega)$ cross-over smoothly from the adiabatic (or quasi-particle) limit at threshold to nearly constant values (~ 0.92 and ~ -0.2 rad, respectively) in the EXAFS, consistent with experiment $S_R^2 \approx 0.9$ [22]. Clearly, our treatment of losses yields significant improvements in amplitude and phase compared to the

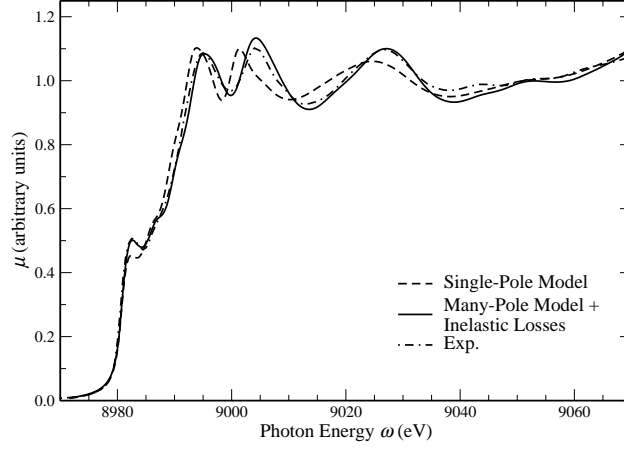


FIG. 3: X-ray absorption μ vs photon energy ω for fcc Cu for our many-pole model with inelastic losses (solid); a single-pole model (dashes); and experiment (dash-dots) [23].

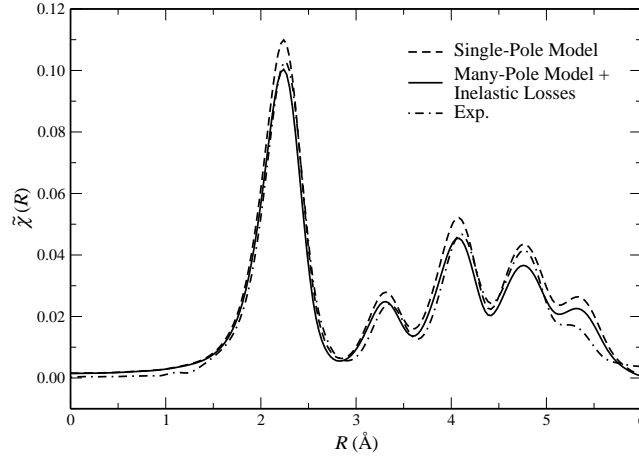


FIG. 4: Fourier transform of the Cu K-edge EXAFS $\tilde{\chi}(R)$ at 10K vs half MS path-length R with (solid), and without inelastic losses (dashes), and from experiment (dash-dots) [23].

single-pole model, both for the near edge spectra (XANES) (Fig. 3) and the EXAFS (Fig. 4). Additional details are given elsewhere [21].

Finally, we present an *ab initio* approach for calculating the effects of vibrational damping on the spectra. Our method is based on calculations of the dynamical matrix \mathbf{D} together with a Lanczos algorithm for the phonon spectra [24, 25]. Instead of relying on spring-constants or semi-empirical approximations, we use first principles electronic structure methods to determine the real space matrix elements of \mathbf{D} ,

$$D_{jl\alpha,j'l'\beta} = (M_j M_{j'})^{-1/2} \frac{\partial^2 U}{\partial u_{jl\alpha} \partial u_{j'l'\beta}}, \quad (6)$$

where U is the total internal energy of the system and $u_{jl\alpha}$ is the $\alpha = \{x, y, z\}$ Cartesian displacement of atom j of mass M_j in unit cell l . The DW factor $\exp(-2\sigma_R^2 k^2)$ for a given MS path R is related to the second cumulant $\sigma_R^2 \equiv \langle (\delta R)^2 \rangle$ of the vibrational distribution function for that path [24],

$$\sigma_R^2(T) = \frac{\hbar}{\mu_R} \int_0^\infty \rho_R(\omega^2) \coth \frac{\beta \hbar \omega}{2} d\omega. \quad (7)$$

Here μ_R is a reduced mass for path R , $\beta = 1/k_B T$ and $\rho_R(\omega^2) \equiv \langle Q_R | \delta(\omega^2 \mathbf{1} - \mathbf{D}) | Q_R \rangle$ is the projected density of phonon modes, which is approximated by a six-step Lanczos recursion, starting from a path displacement seed state $|Q_R\rangle$. Other phonon spectra can be obtained by varying the seed [26]. Although our approach is applicable both to molecules and condensed systems, we present results here only for two crystalline examples. For these systems the $D_{jl\alpha,j'\nu\beta}$ are obtained using ABINIT [27]. Briefly, the reciprocal-space dynamical matrix $\tilde{D}_{j\alpha,j'\beta}(\mathbf{q})$ [28] is calculated on a $4 \times 4 \times 4$ grid of \mathbf{q} -points and smoothly interpolated within the Brillouin zone. The real-space force constants (i.e., second derivatives of U) are then obtained from an inverse Fourier transform. These calculations use Troullier-Martins-FHI pseudopotentials [29] with energy cutoffs of 60 and 15 Hartrees for Cu and Ge respectively, while an $8 \times 8 \times 8$ Monkhorst-Pack grid is used for the electronic energies. Table I presents results obtained with local density approximation (LDA) [31] and generalized gradient approximation (GGA) [32] functionals. The results all lie within about $\pm 10\%$ of experiment [30], with the LDA usually closer. For comparison we show results for the correlated Debye (CD) model [2], which works well for Cu, but gives significant errors for anisotropic structures like Ge. We also calculate anharmonic corrections. The first cumulant is obtained from the net thermal expansion yielding 0.0217 Å for fcc Cu at 300K, in accord with the experimental value 0.0205 ± 0.0009 Å [33]. The third cumulant is then estimated from relations among the cumulants [34]. Further details are given elsewhere [26].

In summary, we have developed efficient, *ab initio* approaches for calculations of the key many-body damping factors in core-level x-ray and electron spectroscopies. Our calculations of inelastic losses are based on a many-pole representation of the dielectric function and an extension of our RSGF code that includes corrections to the independent-particle approximation. This approach yields significantly improved self-energies compared to single-pole models, as well as quantitative IMFPs and estimates of losses due to multi-electron excitations. We have also developed an efficient approach for calculations of phonon spectra

TABLE I: Debye-Waller factors (in 10^{-3} \AA^2) for fcc Cu and dia Ge at 295K for leading near-neighbor shells.

Cu				
Shell	LDA	GGA	CD	Exp. [30]
1	8.55	7.15	8.91	7.93 ± 0.16
2	11.06	9.50	10.99	11.08 ± 0.50
3	10.80	9.14	11.32	9.58 ± 0.60
Ge				
Shell	LDA	GGA	CD	Exp. [30]
1	3.77	3.41	5.12	3.5 ± 0.15
2	10.21	11.59	7.43	9.3 ± 1.1

and MS DW factors. All of these many-body effects are important in applications to optical constants over a broad spectrum, and yield improved amplitudes and phases from the UV to x-ray energies [13]. Since our approach includes solid state effects (e.g., edge shifts, fine structure, and temperature dependent DW factors) and is applicable to general aperiodic materials, these results complement and can potentially replace empirical tables [10, 11, 35, 36, 37] or atomic models [38] for many applications. Extensions, e.g, to spectra at finite momentum transfer and to the visible regime with improved potentials are in progress.

We wish to thank G. Bertsch, C. Chantler, X. Gonze, H. Krappe, H. Lawler, Z. Levine, C. Powell, G. Rivas, H. Rossner, E. Shirley, A. Soininen, and Y. Takimoto for comments and suggestions. This work is supported in part by the DOE Grant DE-FG03-97ER45623 (JJR, MPP) and DE-FG02-04ER1599 (FDV), NIH NCRR BTP Grant RR-01209 (JJK), and NIST Grant 70 NAMB 2H003 (APS) and was facilitated by the DOE Computational Materials Science Network.

[1] G. Onida, L. Reining, and A. Rubio, Rev. Mod. Phys. **74**, 601 (2002).

- [2] J. J. Rehr and R. C. Albers, Rev. Mod. Phys. **72**, 621 (2000).
- [3] J. A. Soininen and E. L. Shirley, Phys. Rev. B **64**, 165112 (2001).
- [4] A. L. Ankudinov, Y. Takimoto, and J. J. Rehr, Phys. Rev. B **71**, 165110 (2005).
- [5] C. J. Powell and A. Jablonski, J. Phys. Chem. Ref. Data **28**, 19 (1999).
- [6] J. M. Fernandez-Varea, F. Salvat, M. Dingfelder, and D. Liljequist, Nucl. Instr. and Meth. B **229**, 187 (2005).
- [7] W. von der Linden and P. Horsch, Phys. Rev. B **37**, 8351 (1988).
- [8] E. E. Krasovskii, W. Schattke, V. N. Strocov, and R. Claessen, Phys. Rev. B **66**, 235403 (2002).
- [9] A. Zangwill and P. Soven, Phys. Rev. A **21**, 1561 (1980).
- [10] H. J. Hagemann, W. Gudat, and C. Kunz, J. Opt. Soc. Am. **65**, 742 (1975).
- [11] B. L. Henke, E. M. Gullikson, and J. C. Davis, At. Data Nucl. Data Tables **54**, 181 (1993).
- [12] M. P. Prange, G. Rivas, J. J. Rehr, and A. L. Ankudinov, unpublished.
- [13] M. P. Prange, G. Rivas, and J. J. Rehr, *Tables of Optical Constants* (WWW, <http://leonardo.phys.washington.edu/feff/opcons/>, 2005).
- [14] J. J. Rehr, J. A. Soininen, and E. L. Shirley, Physica Scripta **T115**, 207 (2005).
- [15] L. Hedin and S. Lundqvist, Solid State Phys. **23**, 1 (1969).
- [16] B. Lundqvist, Phys. Kondens. Materie **6**, 193 (1967).
- [17] J. A. Soininen, A. L. Ankudinov, and J. J. Rehr, Phys. Rev. B **72**, 045136 (2005).
- [18] J. A. Soininen, J. J. Rehr, and E. L. Shirley, J. Phys.: Condens. Matter **15**, 2572 (2003).
- [19] I. Campillo, J. M. Pitarke, A. Rubio, E. Zarate, and P. M. Echenique, Phys. Rev. Lett. **83**, 2230 (1999).
- [20] C. M. Kwei, Y. F. Chen, C. J. Tung, and J. P. Wang, Surf. Sci. **293**, 202 (1993).
- [21] J. J. Kas, L. W. Campbell, M. P. Prange, J. J. Rehr, and A. P. Sorini, unpublished.
- [22] L. W. Campbell, L. Hedin, J. J. Rehr, and W. Bardyszewski, Phys. Rev. B **65**, 064107 (2002).
- [23] M. Newville, Ph.D. thesis, University of Washington (1994).
- [24] A. Poiarkova and J. J. Rehr, J. Synchrotron Radiat. **8**, 313 (2001).
- [25] H. J. Krappe and H. H. Rossner, Phys. Rev. B **66**, 184303 (2002).
- [26] F. D. Vila, H. J. Krappe, H. H. Rossner, and J. J. Rehr, unpublished.
- [27] X. Gonze, J.-M. Beuken, R. Caracas, F. Detraux, M. Fuchs, G.-M. Rignanese, L. Sindic, M. Verstraete, G. Zerah, F. Jollet, et al., Computational Materials Science **25**, 478 (2002).

- [28] X. Gonze and C. Lee, Phys. Rev. B **55**, 10355 (1997).
- [29] M. Fuchs and M. Scheffler, Comput. Phys. Commun. **119**, 67 (1999).
- [30] E. A. Stern, B. A. Bunker, and S. M. Heald, Phys. Rev. B **21**, 5521 (1980).
- [31] J. P. Perdew and Y. Wang, Phys. Rev. B **45**, 13244 (1992).
- [32] J. P. Perdew, K. Burke, and M. Ernzerhof, Phys. Rev. Lett. **77**, 3865 (1996).
- [33] P. Fornasini, S. a Beccara, G. Dalba, R. Grisenti, A. Sanson, M. Vaccari, and F. Rocca, Phys. Rev. B **70**, 174301 (2004).
- [34] A. I. Frenkel and J. J. Rehr, Phys. Rev. B **48**, 585 (1993).
- [35] E. D. Palik, ed., *Handbook of Optical Constants of Solids* (Academic Press, Orlando, 1985).
- [36] C. T. Chantler, J. Phys. Chem. Ref. Data **24**, 71 (1995).
- [37] W. T. Elam, B. D. Ravel, and J. R. Sieber, Rad. Phys. Chem. **63**, 121 (2002).
- [38] D. Liberman, J. T. Waber, and D. T. Cromer, Phys. Rev. **137**, A27 (1965).